

Fig. 1- Sinogram of rod phantom

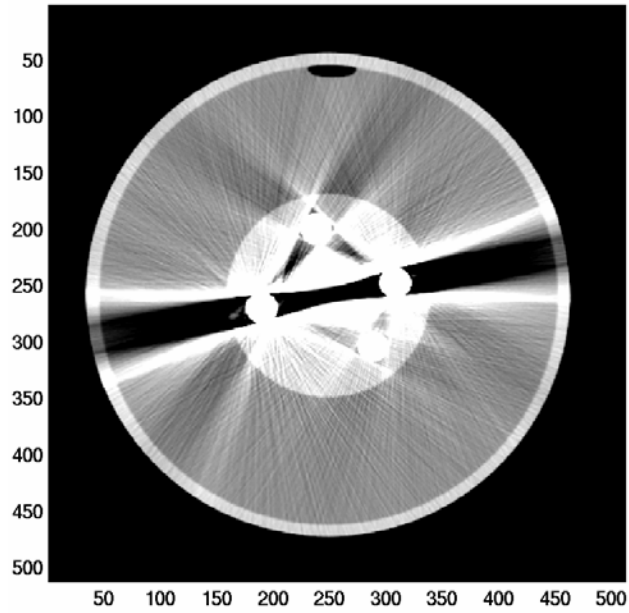


Figure 2. Reconstructed image, showing artifacts. Display set for clinical soft tissue contrast.

		Energy flux	Effective				Linearity
Material	Thickness	flux	Energy	N@E	NEQ	Attenuatio	Error
Air							
Water	20						
Al	1						
Al	2						
W	0.1						
W	0.2						

Table 1. Parameters for CT signals, assuming 120 kVp, 100mAs.

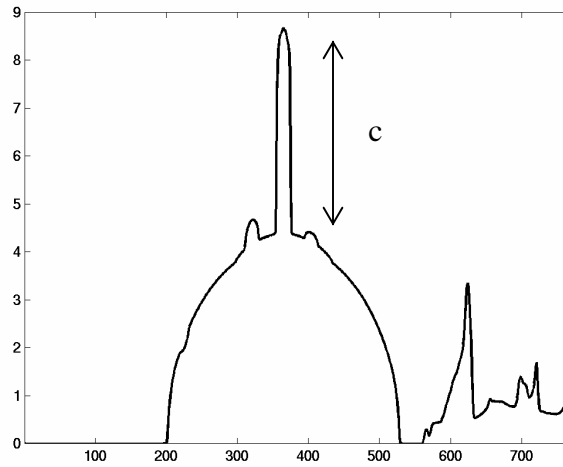
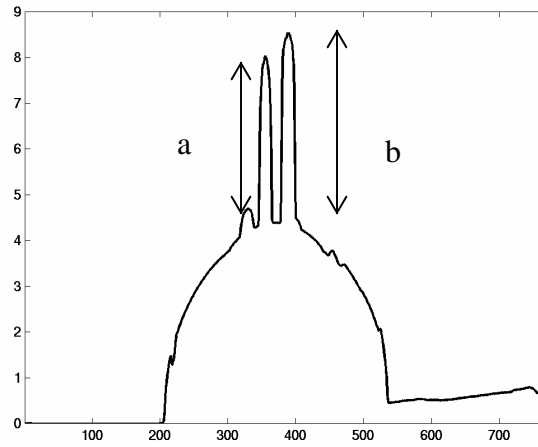


Fig. 3 Top: Vertical profile through gantry column 235, showing non-overlapping rods. Bottom: Vertical profile through gantry column 300, showing overlapping rods. Sum of attenuation is not preserved ($a+b \neq c$).

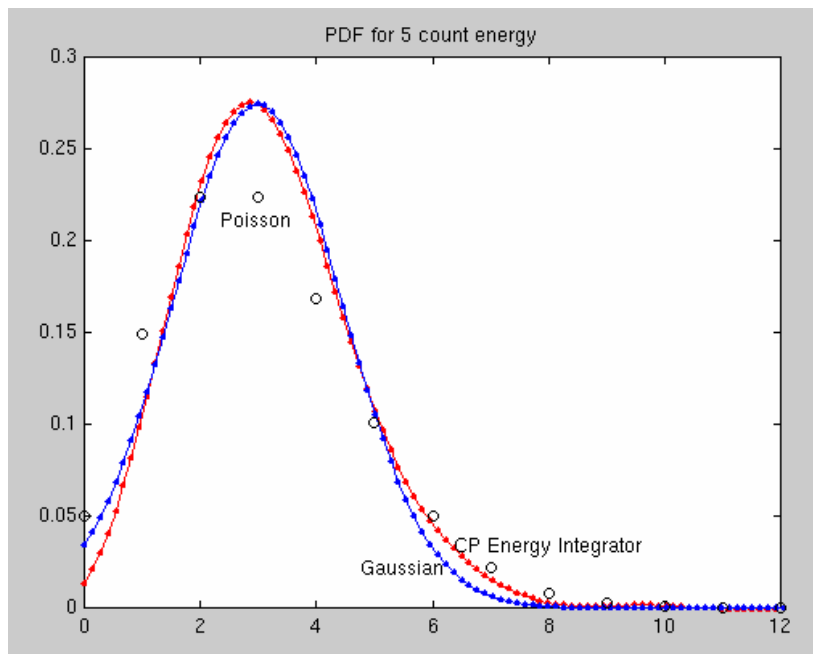
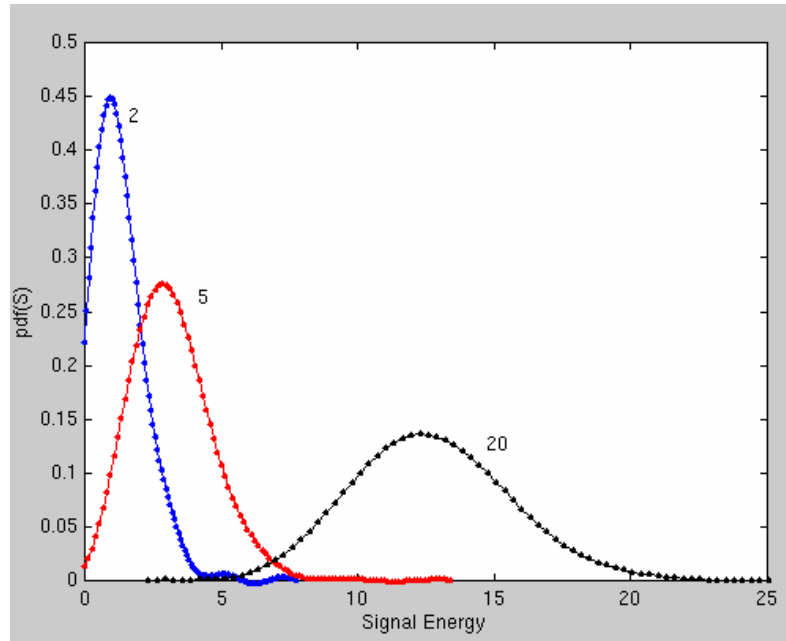


Figure 4. Compound Poisson pdf's for 120kVp with 20 cm water filtration, computed from (5). In upper figure, pdf's for various (arbitrary) signal strengths are plotted. In the lower figure, one of the pdfs has been fitted by a least-squares technique to Poisson and Gaussian distributions.

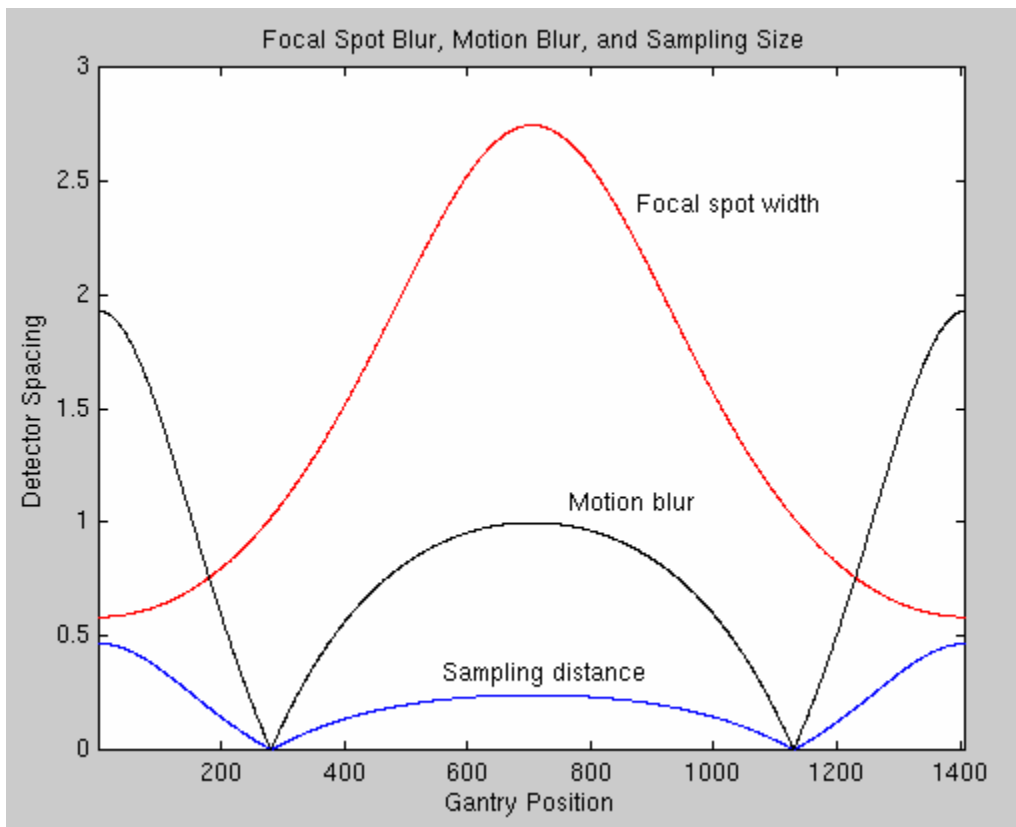


Figure 5- Values of focal spot blur, motion blur and sampling size versus gantry angle for a point 200mm from the isocenter. The blur gives rise to a position dependent point-spread function.

Fig. 6-This will be
schematic of the Fritz
phantom, with beam
stop on side

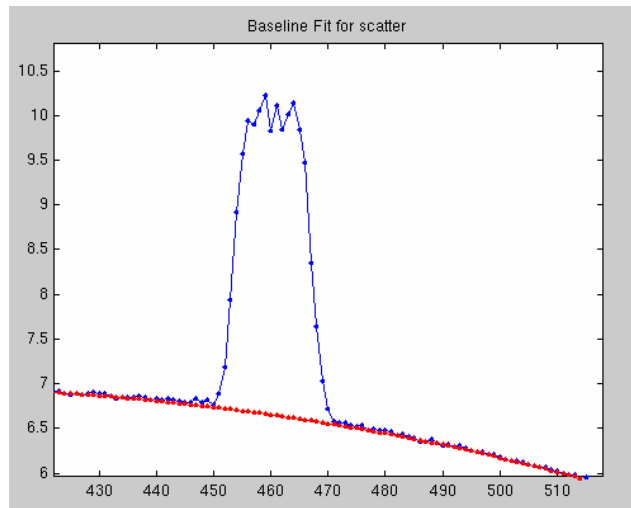
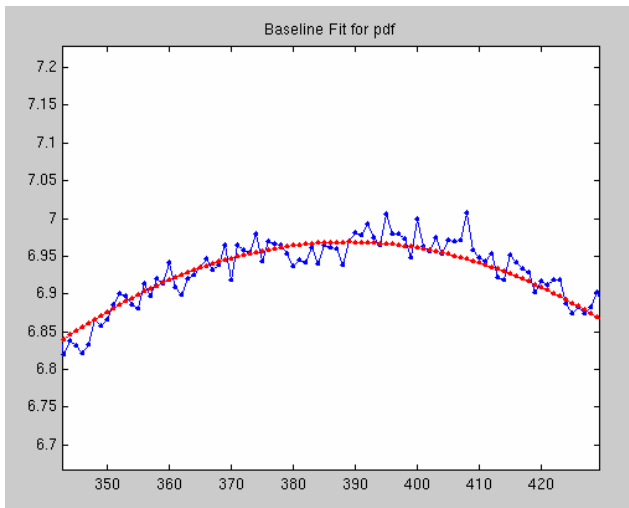
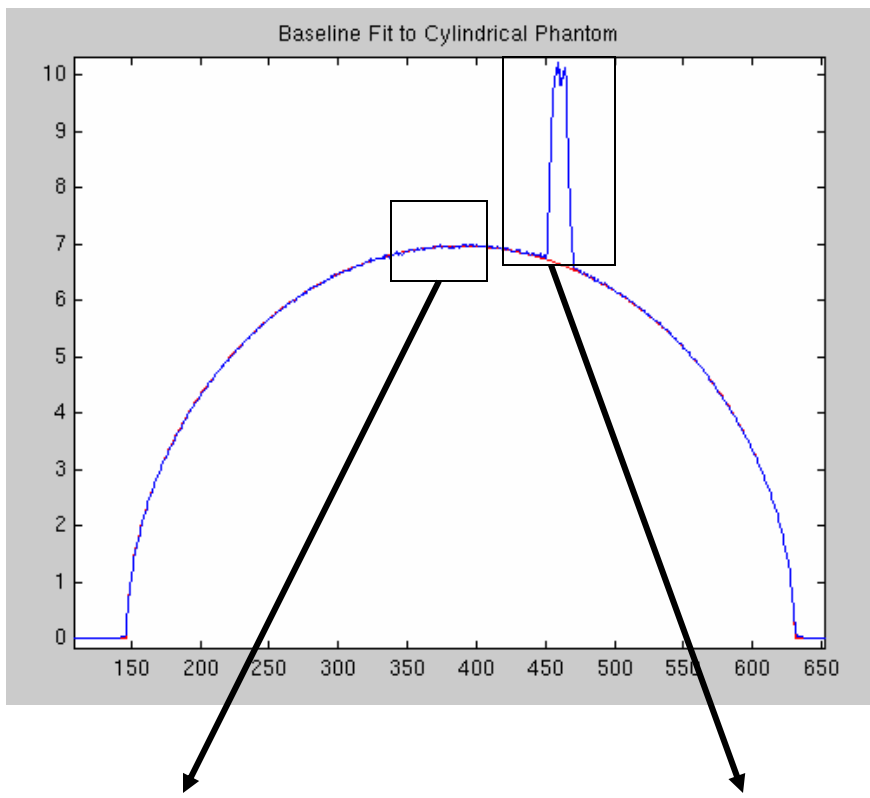


Figure 7- Baseline fitting of phantom to compute pdf and scatter.

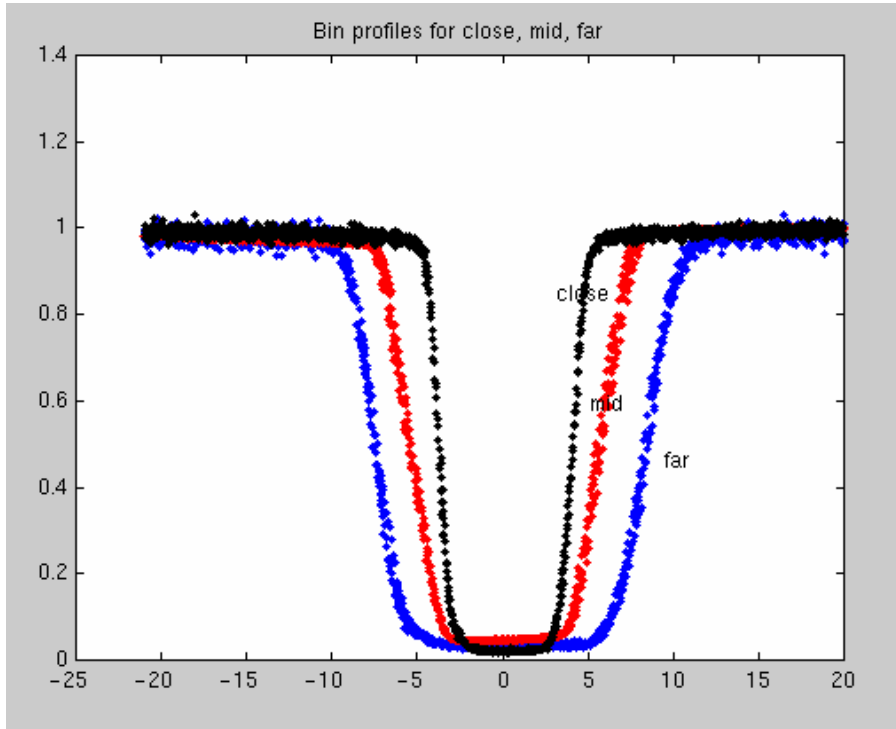


Figure 9- Profiles of beam stop at varying gantry positions. Horizontal axis is in detector units.

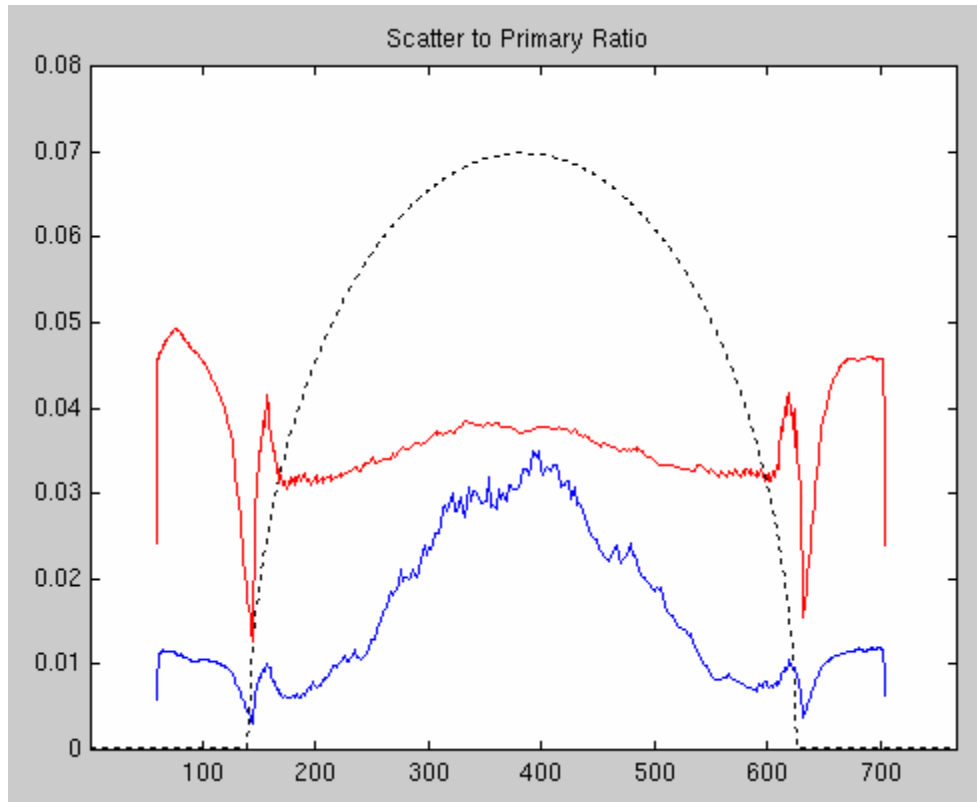


Figure 10- Plots of scatter profile for 1mm (lower) & 10mm (upper) collimations. The attenuation profile (dotted) is provided for reference.

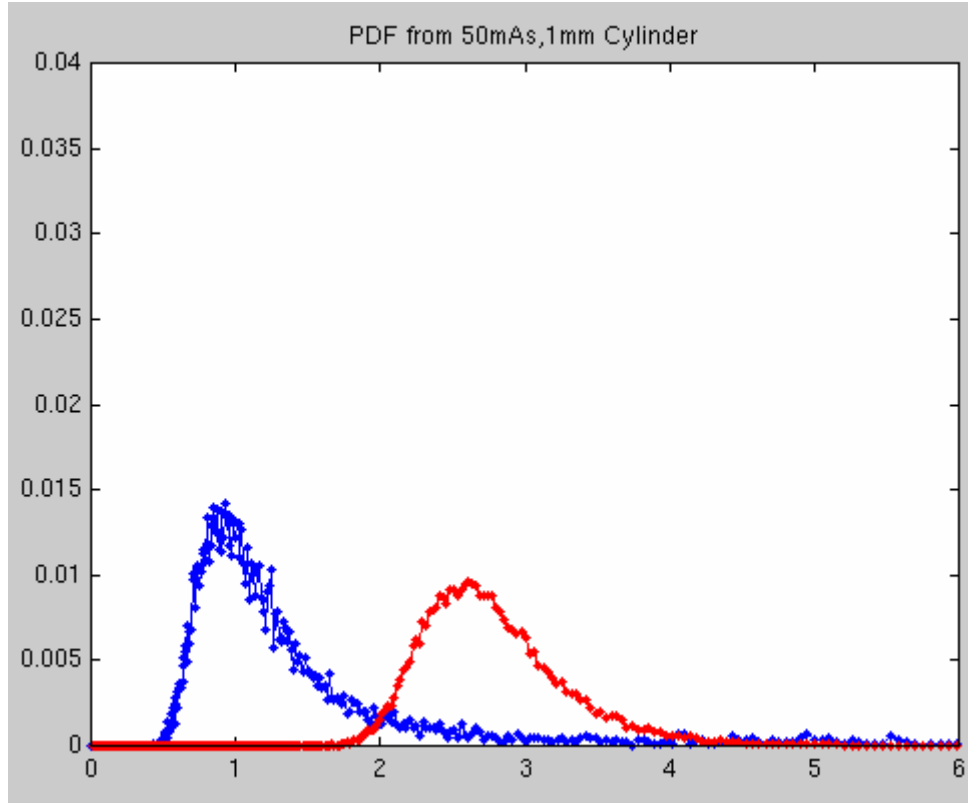


Figure 8- Plots of experimentally measured pdfs from cylinder phantom. From low count regions behind beamstop and on diameter of cylinder.

Figure 11- this will be simulation comparison,
like Lee's.

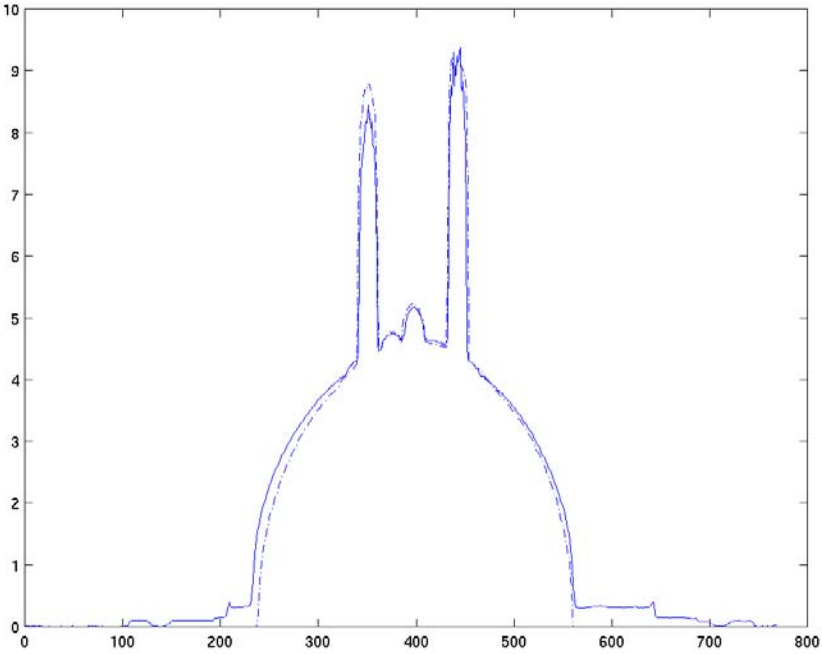


Figure 13- simulations from Dave